2-D Common-Reflection-Surface (CRS) stack based on simulated annealing and quasi-Newton: Application to Marmousi data set

G. Garabito, J.C.R. Cruz, P. Hubral, and M. Tygel

email: *german@ufpa.br*

keywords: *Imaging, Coherency, Optimization*

ABSTRACT

The recently introduced Common-Reflection-Surface (CRS) method is a natural generalization of the well-established Normal Moveout (NMO) method, designed to simulate a zero-offset (ZO) section by a stacking procedure applied to multicoverage data. As opposed to NMO, the stacking procedure in the CRS is not restricted to common-midpoint (CMP) gathers, but uses much more general supergathers of non-symmetrical sources and receivers. Moreover, no selection of interpreted events is required. For the 2D situation considered in this paper, the CRS stacking curve is the general hyperbolic traveltime moveout, that depends on three kinematic wavefield attributes. The crucial step of the CRS method is the estimation of the wavefield attributes at each point of the simulated ZO section to be constructed. This is carried out by means of optimization procedures using as objective function the coherence (semblance) of the seismic traces along the stacking curve. Although a few strategies are already available, the design of accurate and efficient methods to estimate the CRS parameter from the multicoverage data is still a challenging problem.

In this paper we present a solution to this problem that uses a combined approach of global (simulated annealing) and local (quasi-Newton or variable metric) optimization algorithms. The proposed CRS optimization strategy has been applied to the well-known 2-D Marmousi 2-D synthetic seismic data set. The CRS stacked section compared much favorably with the corresponding one obtained using conventional NMO. In addition to the stacked section, we also show and briefly discuss other wavefield-attribute sections that are automatically provided by the CRS method. The obtained results confirm the robustness of the proposed CRS stack algorithm for imaging tectonically complex areas.

INTRODUCTION

During the 1999 the SEG/EAGE Karlsruhe workshop "Macro-model-independent reflection imaging", and in the special issue of the *Journal of Applied Geophysics* edited by Hubral (1999), new imaging approaches were presented with a common characteristic. They were designed to construct an earth image in a data-driven way, without the requirement of an a priori known macro-velocity model. To the proposed methods belong the Multifocusing (MFS) method (Gelchinsky, 1989; Berkovitch et al., 1994; Landa et al., 1999), the Polystack method (de Bazelaire, 1988; de Bazelaire and Viallix, 1994; Thore et al., 1994; Hoecht et al., 1999) and the Common-Reflection-Surface (CRS) method (Mann et al., 1999; Mueller, 1999), the latter being investigated and applied in this paper. The CRS stack is useful to simulate ZO sections by means of a stacking operator that, in the present 2D situation, depends on three parameters: the emergence angle of the normal ray, β_o, and the radii of curvatures R_{NIP} and R_N of two hypothetical wavefronts, so-called Normal-Incidence-Point (NIP) wave and Normal (N) wave, respectively. Both wavefronts are related to second-order paraxial approximations of the reflection traveltime (Hubral and Krey, 1980). The CRS stacking operator is a hyperbolic second-order Taylor expansion of reflection traveltime of a paraxial (finite-offset) ray in the vicinity of a normal (zero-offset) ray. The CRS stack formalism can be extended to include situations for a central ray of finite-offset (Zhang et al., 2001), topography and near-surface

inhomogeneity effects (Chira-Oliva et al., 2001). The data-derived CRS attributes can be used to estimate a macro-velocity model (Biloti et al., 2001).

By using a stratified model with homogeneous layers separated by curved interfaces, Jäger et al. (2001) showed the validity of the CRS stack method to simulate the ZO section and to determine the kinematic wavefield attributes from the multicoverage data. The most impressive application of the CRS stack is found in Bergler et al. (2002) with a real 3-D land data example.

In this paper, following the same CRS formulas as used by Jäger et al. (2001), we present a new procedure for estimating the CRS parameter triplets, β_o, R_{NIP} and R_N, and use it to produce a simulated ZO (stacked) section. Our method is divided into three steps: The first two steps employ a simulated annealing (SA) algorithm, see e.g. Kirkpatrick et al. (1983) and Corona et al. (1987), as a global optimization scheme for obtaining initial estimate of the parameter triplet. The third step refines the previously estimated parameters, by means of a local optimization scheme, the quasi-Newton (QN) algorithm, see e.g. Goldfarb (1970) and Gill et al. (1981). It is important to stress that the proposed strategy can be better suited to handle non-smooth objective functions as is the case of the CRS attribute optimization problem. As in the CRS approach of Jäger et al. (2001), we obtain a CRS stack section, as well as four additional sections, namely the sections of maximum coherence values, emergence angles β_o, and radii of curvatures R_N and R_{NIP}, respectively.

First validation of the proposed SA-QN based CRS procedure has been carried out by (Garabito et al., 001a) and (Garabito et al., 001b) using a simple model of two homogeneous layers separated by smooth interfaces above a half-space. To evaluate the robustness of the SA-QN based CRS algorithm for simulating the ZO section in tectonically complex areas, we now apply it to the well-known Marmousi data set with and without random noise. We confirm that the CRS stack method improves the signal-to-noise ratio of the stacked data and gives rise to clearer stacked sections.

CRS STACK TRAVELTIME APPROXIMATIONS

We start by reviewing the CRS method formalism in the same way as given by Jäger et al. (2001). The 2-D CRS stack hyperbolic second-order Taylor expansion can be derived by means of paraxial ray theory (see, e.g., Schleicher et al. (1993)). It approximates the finite-offset reflection traveltime in the vicinity of a fixed normal ray, generally called a central ray. That ray is specified by its emergence point, x_0, called the central point and generally taken as a CMP. The traveltime of the ZO central ray that pertains to x_o is denoted t_o. It is also assumed that the near-surface velocity, v_0, at the central point, x_0, is known and constant in its vicinity. For a given point, $P_o = (x_o, t_o)$ in the simulated ZO section to be constructed, we consider the CRS stack operator

$$t^2(x_m, h) = \left(t_0 + \frac{2\sin\beta_0}{v_0}(x_m - x_0) \right)^2 + \frac{2t_0\cos^2\beta_0}{v_0}\left(\frac{(x_m - x_0)^2}{R_N} + \frac{h^2}{R_{NIP}} \right). \quad (1)$$

As indicated above, x_o and t_0 denote the emergence point of the normal ray on the seismic line, the central point, and its ZO traveltime, respectively; x_m and h midpoint and half-offset coordinates

$$x_m = (x_s + x_r)/2 \text{ and } h = (x_s - x_r)/2, \quad (2)$$

where x_s and x_r are the coordinates of the source and receiver on a planar acquisition surface. The seismic line is considered to coincide with the horizontal Cartesian coordinate axis, x, along which x_s, x_r and x_o are specified. The point $P_o(x_0, t_0)$ in the ZO section to be simulated is the one in which is assigned the stacked seismic amplitudes with formula (1).

In the case that the reflector element collapses into a diffractor point, the wavefronts NIP and Normal coincide. As a consequence, $R_{NIP} = R_N$ so that the formula (1) reduces to

$$t^2(x_m, h) = \left(t_0 + \frac{2\sin\beta_0}{v_0}(x_m - x_0) \right)^2 + \frac{2t_0\cos^2\beta_0}{v_0}\left(\frac{(x_m - x_0)^2 + h^2}{R_{NIP}} \right). \quad (3)$$

Formula (3) is the Common-Diffraction-Surface (CDS) stack operator. It is an approximation of the pre-stack Kirchhoff migration operator in the vicinity of $P_o(x_o, t_o)$. The CDS stack operator is the one

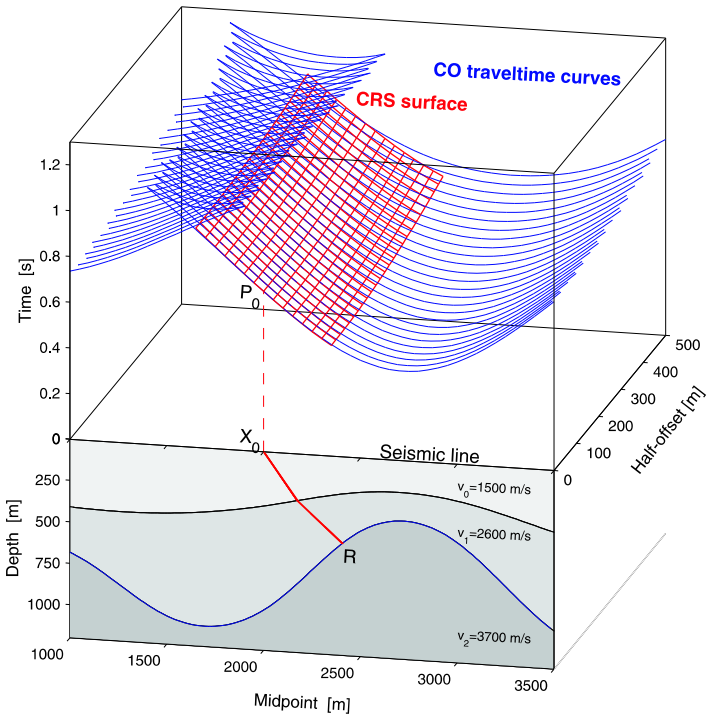

Figure 1: *Upper half:* CRS stack operator for point P_o in the ZO seismic section. *Lower half:* Model with two homogeneous layers above a half-space separated by a curved interface.

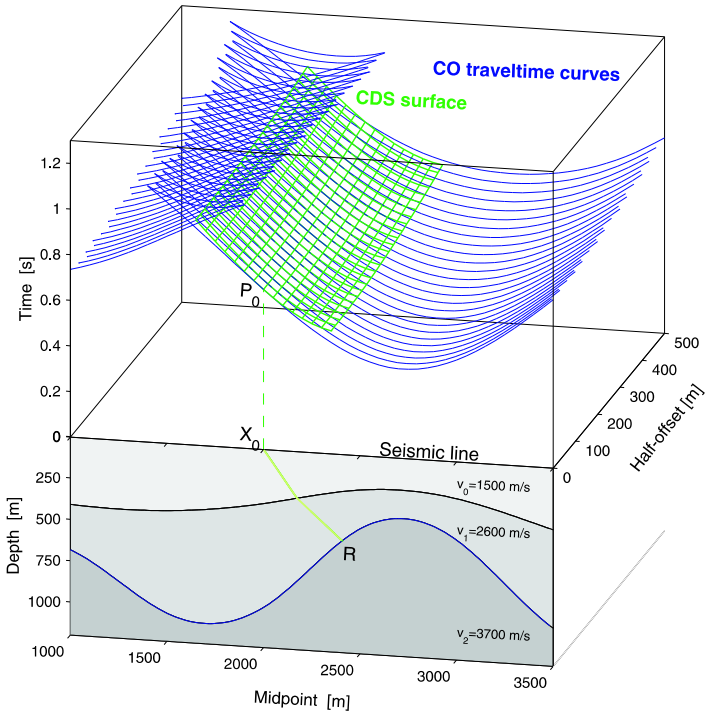

Figure 2: *Upper half:* CDS stack operator for point P_o in the ZO seismic section. Lower half: Model with two homogeneous layers above a *half-space* separated by a curved interface.

used to simultaneously estimate the two parameters β_0 and R_{NIP}, as a first step of the new CRS parameter estimation strategy proposed in this work.

Another important special case results from setting $h = 0$ in the traveltime formula (1), namely

$$t^2(x_m, h) = \left[t_0 + \frac{2 \sin \beta_0}{v_0}(x_m - x_0) \right]^2 + \frac{2 t_0 \cos^2 \beta_0}{v_0} \left[\frac{(x_m - x_0)^2}{R_N} \right]. \quad (4)$$

This is the situation of ZO reflection traveltimes in the vicinity of the ZO central ray. As shown below, equation (4) will be used to determine the parameter R_N at the second step of our proposed estimation strategy.

For a simple model of two layers and curved interfaces, Figure 1 depicts the CRS stack operator (CRS surface) and the multi-coverage reflection traveltime surface (common-offset (CO) traveltime curves) in the (x_m, h, t)-domain. Figure 2 depicts the corresponding CDS stack operator (that is, under condition $R_{NIP} = R_N$) for the same reflection point R of Figure 1. The CRS stack aperture is a region in the (x_m, h)-plane in the vicinity of the central point $(x_o, 0)$, where the estimation procedure is performed to find the CRS stacking parameters. The hyperbolic traveltime surface of equation (1) approximates the modelled traveltime surface within that region.

An important aspect of the general traveltime formula (1) is that it can be reduced to different mathematical expressions for specific applications. These depend on the relation between R_N and R_{NIP}, the chosen data configuration (e.g. common-shot, common-offset, ZO, common-receiver, common-midpoint, 2-D or 3-D), the measurement surface topography and near-surface heterogeneity.

OPTIMIZATION PROCESS

The objective function of the CRS method is the coherence (semblance) of the amplitudes along and in the vicinity of the CRS surface (1). The optimization procedure is automatically carried out for each point $P_o(x_o, t_o)$ in the simulated ZO section. The inverse problem to be solved is stated as follows: To search for the parameter triplet that maximizes the semblance along the corresponding CRS traveltimes. A particular difficulty is that we have in many situations more than one maxima and we need to consider, in addition to the global maximum, also a couple of (local) maxima. This case arises when there are conflicting dips in the ZO section. The present SA-QN algorithm used in this work is able to consider, besides the global, also one additional local maximum, using both to stack the seismic data.

2-D SA-QN BASED CRS STACK: A NEW APPROACH

The CRS strategy used by Jäger et al. (2001) starts from a so-called automatic stack that consists of a coherence analysis applied to each CMP gather and each ZO time sample. The automatic stack determines the combined stack parameter $q = \dfrac{\cos^2 \beta_o}{R_{NIP}}$. As a next step, using an automatic post-stack procedure, a first estimation of the CRS parameters β_o and R_N are obtained; together with the previously obtained combined parameter, q, an initial guess of the three CRS parameters is obtained. Finally, the estimated parameter triplet is refined by a full, three-dimensional optimization procedure. After this scheme is carried out for each central point and each ZO time sample, an optimized CRS stack section and its corresponding optimized CRS parameter sections are obtained.

In this paper, we propose a new procedure to estimate the three CRS parameters β_o, R_{NIP} and R_N, by combining SA and QN optimization methods. The scheme, that also consists of three steps, is outlined by the flowchart of Figure 3. Upon the consideration of a fixed point $P_o(x_o, t_o)$ at the ZO section to be simulated, the proposed three steps can be briefly described as follows:

Step I : Pre-Stack Global Optimization

This step uses a multi-coverage pre-stack seismic data as input, and the common-diffraction-surface (CDS) traveltime equation (3) as stack operator. The task is to simultaneously estimate the best parameters β_0 and R_{NIP} that yield the maximum semblance value. To solve the problem, we use a global optimization SA algorithm. To start the algorithm, we consider random values extracted from a priori defined intervals (so-called physical intervals) into which the CRS parameters are divided. The procedure is repeated for all points P_o of the ZO section to be simulated. The following resulting sections are obtained: 1) Maximum

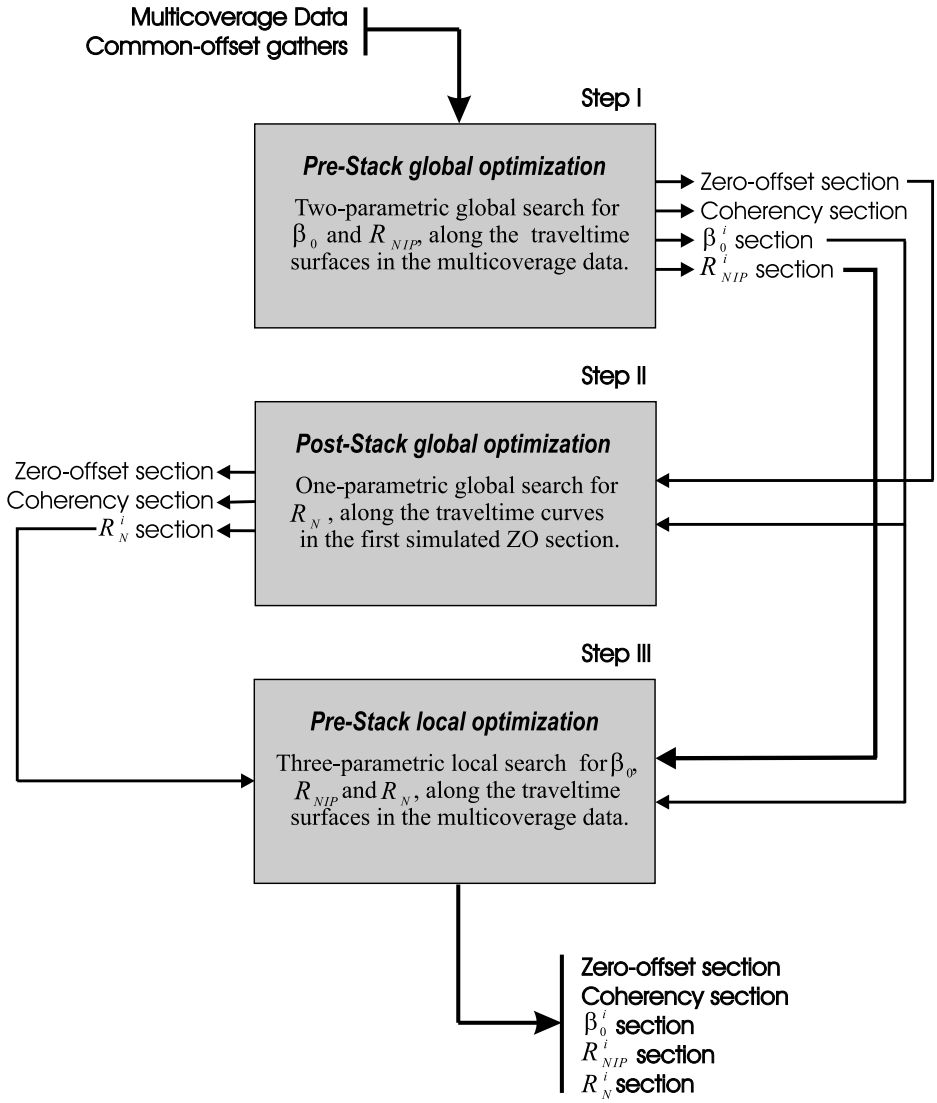

Figure 3: Flowchart of the SA-QN based CRS stack procedure with three steps. They are sequentially performed by using respectively formulas (3), (4) and (1).

coherence section; 2) Emergence angle section; 3) Radius of curvature of NIP wavefront section and 4) Simulated ZO section.

Step II : Post-Stack Global Optimization

This step uses the post-stack (simulated ZO section) seismic data as input, and the ZO stack operator expressed by formula (4). Under the assumption that the previously obtained β_o is kept fixed, the procedure consists of a one-dimensional search for the parameter R_N, that corresponds to the maximum semblance value. After repeating this procedure for all points P_o of the ZO section to be simulated, we have the following results: 1) Maximum coherence section; 2)Radius of curvature of N-wavefront section and 3) an improved ZO section.

Step III : Pre-Stack Local Optimization

This step uses the full multi-coverage pre-stack seismic data as input, and the CRS stack operator of equation (1). The inverse problem is then to estimate the parameter triplet (β_0, R_{NIP}, R_N) that maximizes the semblance value. At this stage, we make use of the local optimization QN algorithm, in which the previously estimated CRS parameters are taken as initial values. After repeating this procedure for all points

P_o of the ZO section to be simulated. The following final results are obtained: 1) Maximum coherence section; 2) Emergence angle section; 3) Radius of curvature of the NIP wavefront section; 3) Radius of curvature of the Normal wavefront section and 4) Final simulated ZO section.

APPLICATION

To study the performance of the CRS stack procedure proposed in this paper, we applied it to the well-known Marmousi data set (Bourgeois et al., 1991).

The Marmousi experiment is a synthetic data computed on a model with highly complex structures and tectonically realistic distribution of reflectors. The model contains 60 reflectors of steep dips and strong velocity gradients in both vertical and horizontal directions. The profiles were registered by marine technique shooting from west to east. The seismic data set consists of 240 shots, each shot with 96 traces and each trace with 725 samples. The sampling interval is 4 ms and both source - and - receiver separations are 25 m. The minimum offset is 200 m. The first shot point is located at 3000 m from the west edge of the model.

The CRS stack proposed here is fully automatic, namely no interference on the processing flow is required from the user. In addition, the input seismic data used in the CRS stack was not submitted to any pre-processing. The full multicoverage data, with particular inclusion of traces from asymmetric source-receiver locations with respect to central points, have been used.

Figure 4 shows the CRS stack section as obtained by the procedure described above. For comparison, we show in Figure 5 the corresponding section that results from conventional NMO/DMO stacking. We see that the CRS stack provides a better ZO section in the deeper zones of the Marmousi model, even in the most complex regions. Horizons localized in the central part of the stacked section deserve particular attention. In the CRS staked section they are more enhanced as compared with their counterparts in the NMO/DMO section. This provides a good indication that the CRS stack method can help to improve time-or depth-migrated seismic image in tectonically complex areas.

Figure 6 shows the section of semblance values after final optimization. For the sake of completeness, we present Figures 7, 8 and 9 that show the CRS parameter sections β_0, R_{NIP} and R_N, respectively. Evaluation of the obtained CRS attribute sections would require the consideration of some geologic features of the Marmousi model, so as, for instance, to relate the attributes to identified reflectors. Moreover, comparison with the CRS method implementation, as in Mueller (1999); Jäger et al. (2001), would also be adequate.

As our focus here is mainly to describe the new CRS method optimization strategy, as done above, we refrain to discuss on the CRS attribute sections, presenting them just as illustrations of the proposed CRS procedure. It is important, however, to stress the value of the semblance and CRS parameter sections to derive additional wave-propagation attributes, such as NMO velocities, geometrical-spreading factors and Fresnel zones (see, e.g., Jäger et al. (2001)).

We also tested ability of the CRS stack process to process noisy data. Figure 10 shows the CRS stack that results from the previous Marmousi data in which random noise has been applied, with a signal-noise ratio of S/N=3. The result is compared with an original (noisy) near-offset section (200 m) of Marmousi data set, shown in Figure 11. The significantly higher signal-to-noise ratio in the CRS stack section is to be observed.

CONCLUSIONS

In this paper we proposed a new procedure for estimating the three parameters in the CRS stack method: The first two steps use the global optimization method of simulating annealing (SA). The third step uses the quasi-Newton (QN) algorithm, a local optimizer. The result is an efficient way to obtain accurate CRS attributes and, as a consequence, an improved simulated ZO section. We applied the new CRS stack procedure to the Marmousi data set. The CRS stacked section showed significantly enhanced reflections, as compared with the NMO/DMO stack. The CRS stack also performed very well in the presence of random noise added to the original data set. The obtained results indicates that the CRS is able to provide clear ZO sections also in tectonically complex areas. Besides producing stacked sections with enhanced signal-to-noise reflections, the CRS method also provides three additional attribute sections that are useful to a variety of seismic processing tasks, including the estimation geometrical-spreading factors, Fresnel zones and the inversion of velocity models.

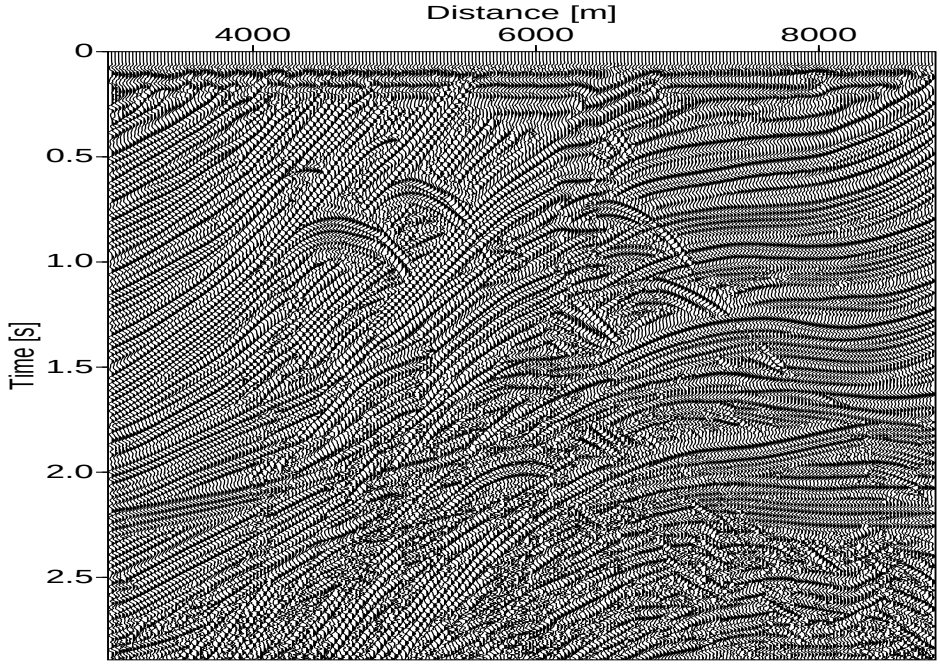

Figure 4: Simulated ZO section by the CRS stack method having as input the Marmousi data set.

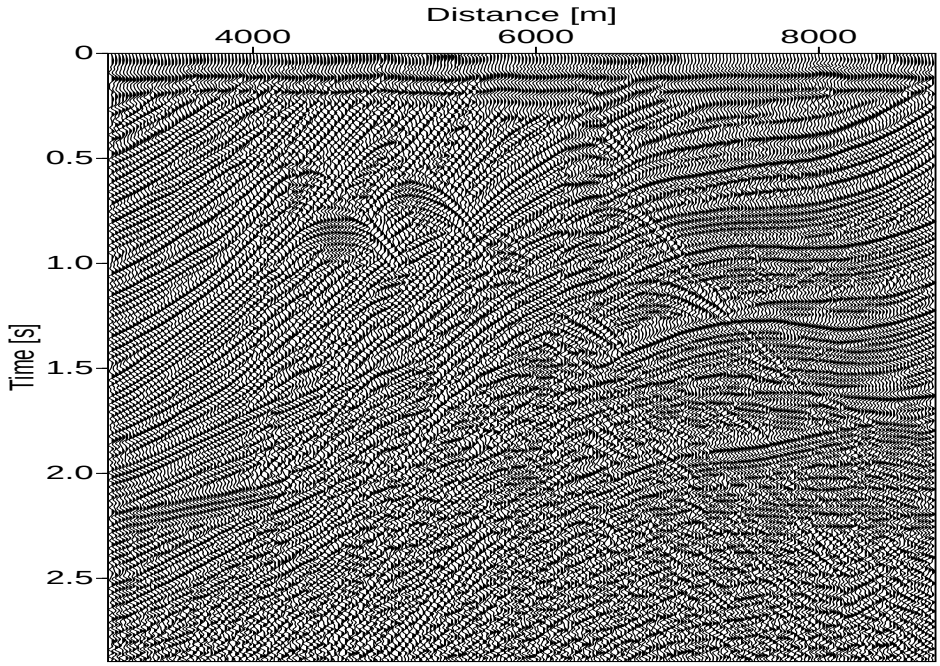

Figure 5: Simulated ZO section by the NMO/DMO stack method having as input the Marmousi data set.

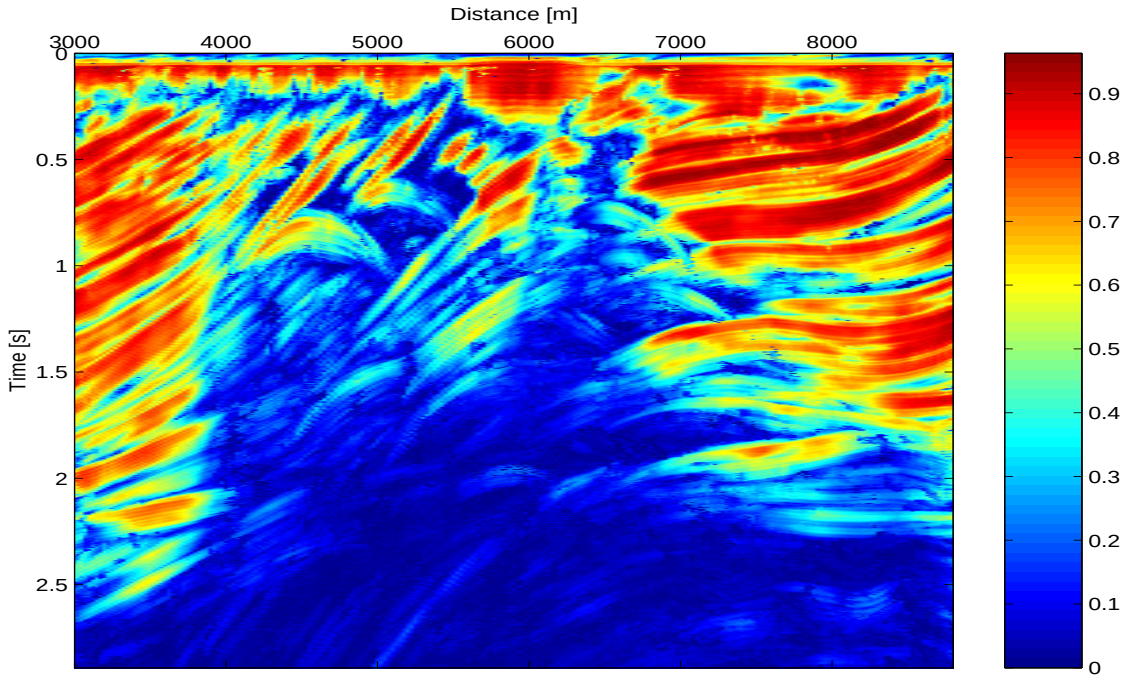

Figure 6: Section with the maximum semblance values obtained from applying the CRS algorithm to the Marmousi data set.

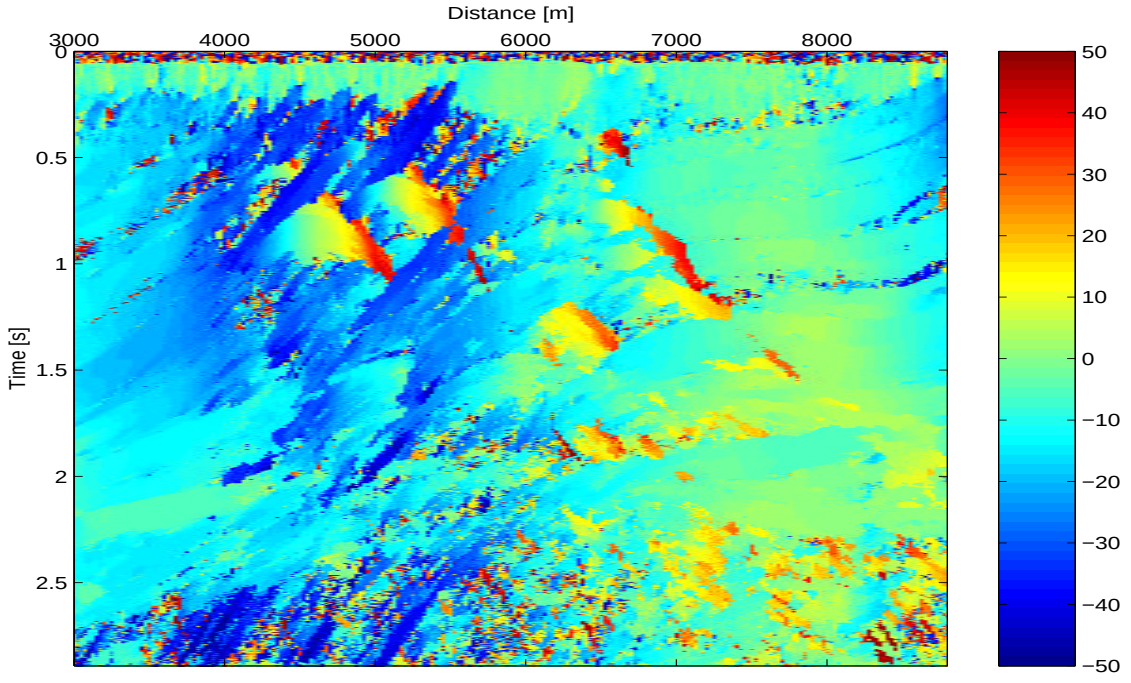

Figure 7: Section with the emergence angles of normal rays, β_o, estimated from the CRS stack applied to the Marmousi data set.

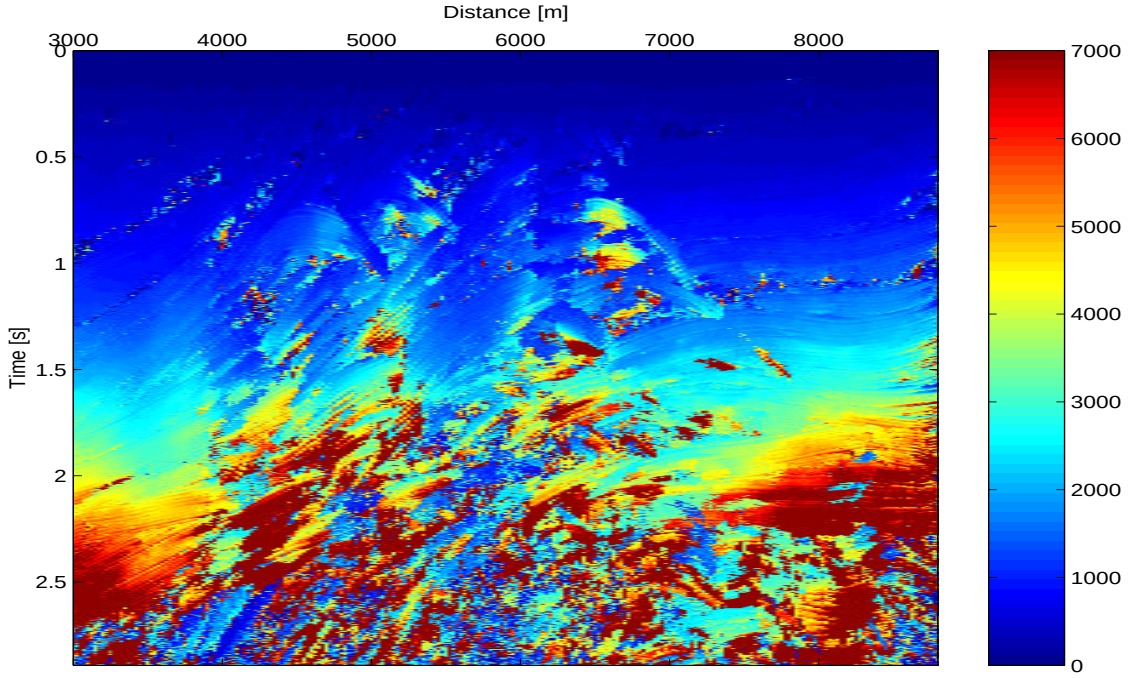

Figure 8: Section with the radius of curvature of NIP wavefronts, R_{NIP}, estimated from the CRS stack applied to the Marmousi data set.

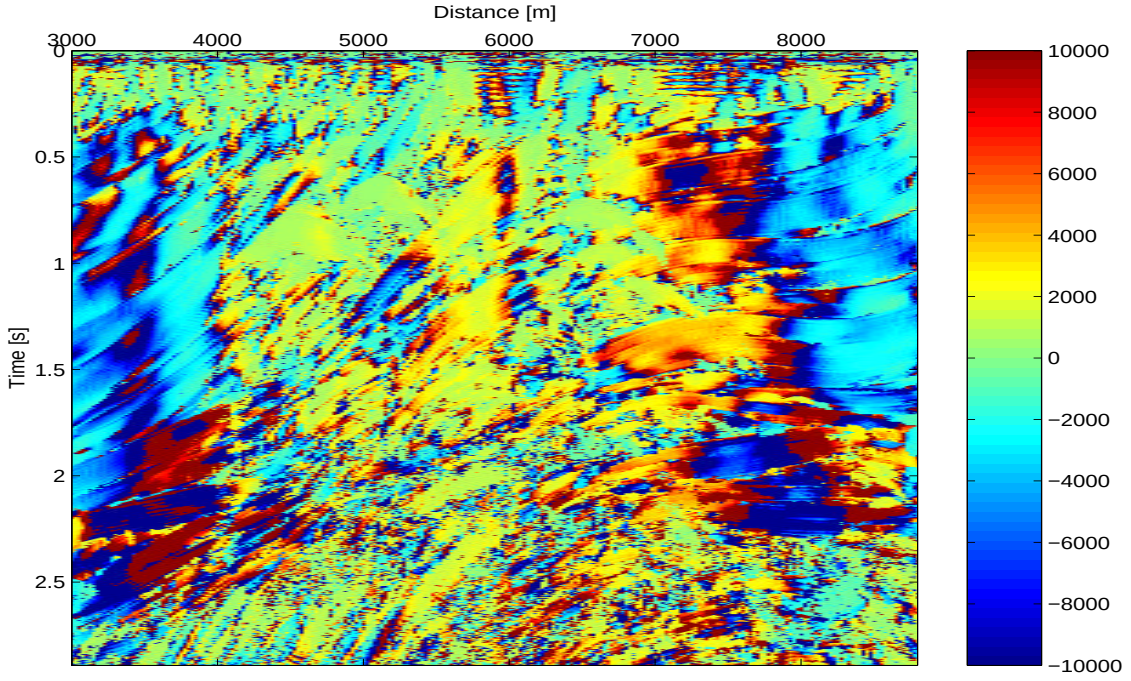

Figure 9: Section with the radius of curvature of Normal wavefronts, R_N, estimated from the CRS stack applied to the Marmousi data set.

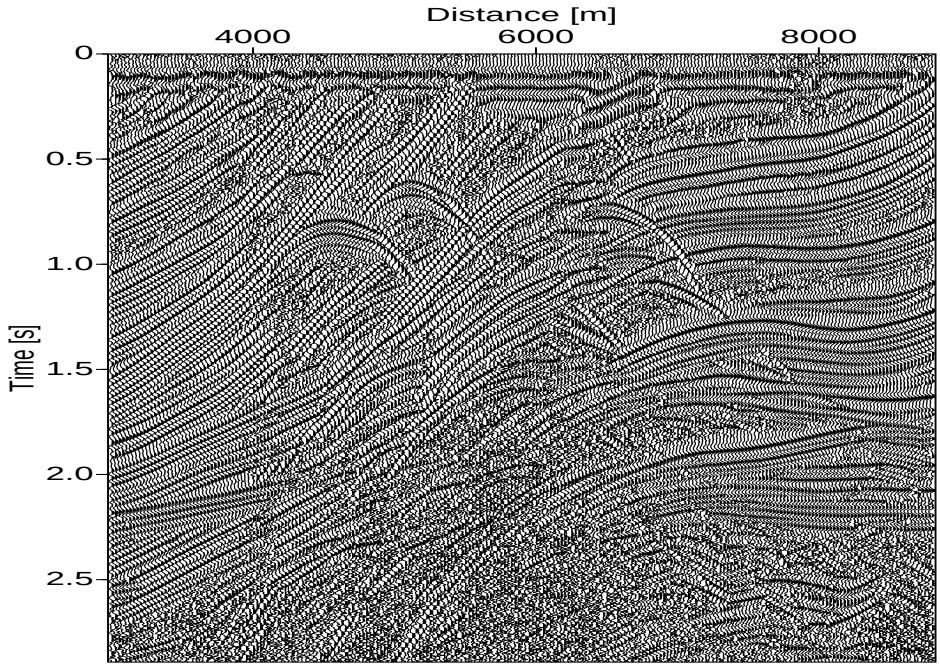

Figure 10: Simulated ZO section by CRS stack method having as input the Marmousi data set with random noise added.

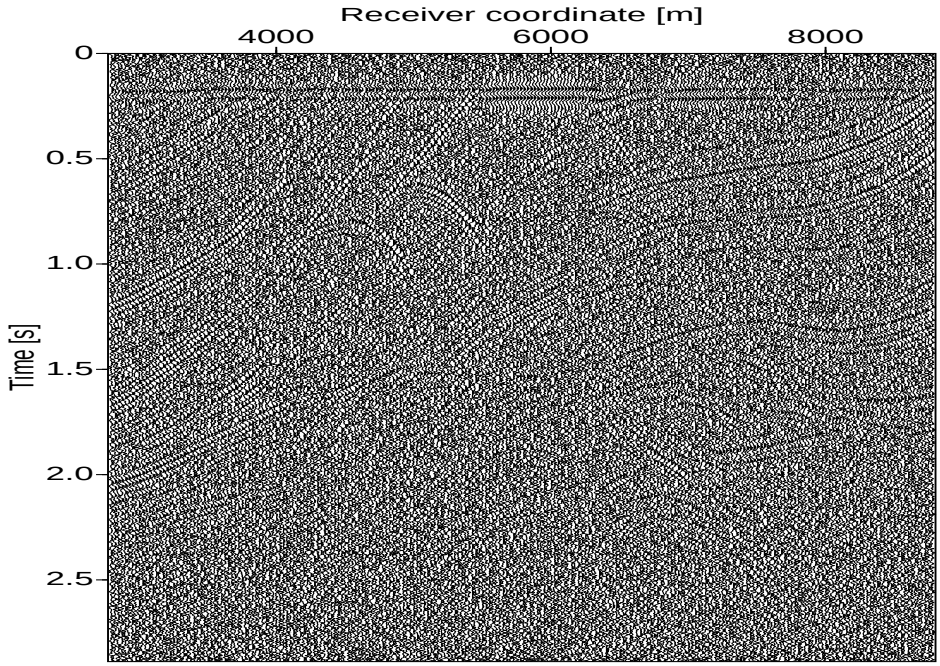

Figure 11: Near offset section (200 m) of Marmousi data set with random noise.

PUBLICATIONS

The first results of the proposed SA-QN based CRS stack procedure has been carried out by (Garabito et al., 001a) and (Garabito et al., 001b), using a simple model of two homogeneous layers separated by smooth interfaces.

ACKNOWLEDGMENTS

The first author thanks the National Petroleum Agency (ANP-Brazil) and the National Council for Scientific and Technological Development (CNPq-Brazil) for scholarships during his doctoral studies at the Federal University of Pará-Brazil. We all thank the support provided by the sponsors of the *Wave Inversion Technology (WIT) Consortium.*

REFERENCES

Bergler, S., Marchetti, P. H. P., Cristini, A., and Cardone, G. (2002). 3d common-reflection-surface stack and kinematic wavefield attributes. *The Leading Edge*, 21(10):1010–1015.

Berkovitch, A., Gelchinsky, B., and Keydar, S. (1994). Basic formulae for multifocusing stack. *56th. Mtg. EAGE, Expanded Abstracts, Session P140.*

Biloti, R., Santos, L., and Tygel, M. (2001). Macro-velocity model inversion from traveltime attributes. *71st. SEG Mtg., San Antonio, USA.*

Bourgeois, A., Bouget, M., Lailly, P., Poulet, M., Ricarte, P., and Versteeg, R. (1991). Marmousi, model and data. *52nd. EAGE mtg., Proceedings of the Workshop on Practical Aspects of Seismic Data Inversion*, pages 5–16.

Chira-Oliva, P., Tygel, M., Zhang, Y., and Hubral, P. (2001). Analytic crs stack formula for a 2d curved measurement surface and finite-offset reflections. *Journal of Seismic Exploration*, 10:245–262.

Corona, A., Marchesi, M., Martini, C., and Ridela, S. (1987). Minimizing multimodal functions of continuous variables with 'simulated annealing' algorithm. *ACM Transactions on Mathematical Software*, 13(3):262–280.

de Bazelaire, E. (1988). Normal moveout revisited-inhomogeneous media and curved interfaces. *Geophysics*, 53:143–157.

de Bazelaire, E. and Viallix, R. J. (1994). Normal moveout in focus. *Geophys. Prosp.*, 42:477–499.

Garabito, G., Cruz, J. C., Hubral, P., and Costa, J. (2001a). Common reflection surface stack: A new parameter search strategy by global optimization. *71th. SEG Mtg., Expanded Abstracts. San Antoinio, Texas,USA.*

Garabito, G., Cruz, J. C., Hubral, P., and Costa, J. (2001b). Common reflection surface stack with conflicting dip (in portuguese). *In Expanded Abstracts. 7th. International Congress of Brazilian Geophysical Society.*

Gelchinsky, B. (1989). Homeomorphic imaging in processing and interpretation of seismic data - fundamentals and schemes. *59th. Mtg. SEG, Expanded Abstracts, 983.*

Gill, P. E., Murray, W., and Wright, M. H. (1981). *Practical Optimization*. Academic Press, London and New York.

Goldfarb, D. (1970). A family of variable metric methods derived by variational means. *Mathematical of Computation*, 24:23–26.

Hoecht, G., de Bazelaire, E., Majer, P., and Hubral, P. (1999). Seismic and optics: Hyperbolae and curvatures. *J. Appl. Geophys.*, 42(3):261–281.

Hubral, P. (1999). Special issue: Macro-model independent seismic reflection imaging. *Journal of Applied Geophysics*, 42:Nos. 3,4.

Hubral, P. and Krey, T. (1980). Interval velocities from seismic reflection time measurements: Monograph. *Soc. Expl. Geophys.*

Jäger, R., Mann, J., Höcht, G., and Hubral, P. (2001). Common reflection surface stack: Image and attributes. *Geophysics*, 66:97–109.

Kirkpatrick, S., Gelatt, C., and Vecchi, M. (1983). Optimization by simulated annealing. *Science*, 220:671–680.

Landa, E., Gurevich, B., Keydar, S., and Trachtman, P. (1999). Application of multifocusing method for subsurface imaging. *J. Appl. Geophys.*, 3:283–300.

Mann, J., Jäger, R., Müller, T., Höcht, G., and Hubral, P. (1999). Common-reflection-surface stack - a real data example. *Journal of Applied Geophysics*, 42:301–318.

Metropolis, N., Rosenbluth, A., Rosenbluth, M., and Teller, A. (1953). Equation of state calculations by fast computing machines. *J. Chem. Phys.*, 21:1087–1092.

Mueller, T. (1999). The common reflection surface stack method - seismic imaging without explicit knowledge of the velocity model. *Ph.D. Thesis, University of Karlsruhe, Germany*.

Schleicher, J., Tygel, M., and Hubral, P. (1993). Parabolic and hyperbolic paraxial two-point traveltimes in 3d media. *Geophys. Prosp.*, 41:495–513.

Sen, M. and Stoffa, P. (1995). *Global Optimization Methods in Geophysical Inversion*. Elsevier, Science Publ. Co.

Thore, D. P., de Bazelaire, E., and Ray, P. M. (1994). Three-parameter equation: An efficient tool to enhance the stack. *Geophysics*, 59:297–308.

Zhang, Y., Bergler, S., and Hubral, P. (2001). Common-reflection-surface (crs) stack for common-offset. *Geophys. Prosp.*, 49:709–718.

APPENDIX A

SIMULATED ANNEALING

Simulated annealing (SA) method is a global optimization scheme designed to solve general nonlinear inverse problems. For an introduction to the SA approach and applications to geophysical problems the reader is referred to Kirkpatrick et al. (1983) and Sen and Stoffa (1995). The SA method is rather robust, allowing for very flexible choices of both the region where the procedure is to be applied, as well as the initial values (generally an automatic choice) of the searched-for parameters from which the method is triggered. Due to its robustness and ease adaptation to the CRS problem, we use in this work an improved implementation of SA algorithm as described in Corona et al. (1987). A brief description of this algorithm it is presented below.

The SA algorithm starts with a CRS parameter vector $\mathbf{m}_0 = (\beta, K_{NIP}, K_N)$, that is chosen at random. As described in the main text, the kinematic reflection traveltime response is then calculated by the CDS equation (3) as a first step, or by the ZO equation (4) as a second step. As a result, the traveltime moveout

$$t_{\mathbf{m}_0} = t(x_m, h; \mathbf{m}_0), \tag{5}$$

is obtained. The above traveltime moveout is defined for a suitable aperture in the (x_m, h)-domain, around the central point, x_0. Using equation (5) as stacking operator, we evaluate the corresponding semblance value,

$$S_{\mathbf{m}_0} = S(x_o, t_o; t_{\mathbf{m}_0}), \tag{6}$$

namely, the objective function to be maximized. Starting from the initial parameter, $\mathbf{m_0}$, a sequence of CRS parameter vectors $\{\mathbf{m_k}\}$, $k = 1, 2, ...$ is now iteratively produced and that is supposed to converge to the global maximum of the objective function. To explain the process, suppose that the parameter vector $\mathbf{m_{k-1}}$ has been already obtained. The new parameter vector, $\mathbf{m}_k$, is generated by perturbing $\mathbf{m}_{k-1}$, with

$$\mathbf{m}_k = \mathbf{m}_{k-1} + r\mathbf{v}, \tag{7}$$

where r is a uniformly distributed random number belonging to $[-1, 1]$ and $\mathbf{v}$ is a step-length vector, which has the same length of parameters vector $\mathbf{m}$.

This produces a corresponding new semblance value, $S_{\mathbf{m}_k}$. Next, the semblance difference $\Delta S_k = S_{\mathbf{m}_{k-1}} - S_{\mathbf{m}_k}$ is considered. If it is zero or negative, the new CRS parameter vector is accepted, meaning that the overall fit between the CRS stack operator and the multi-coverage seismic data has improved after the CRS parameter vector perturbation. For a positive ΔS_k, however, the vector parameter, $\mathbf{m}_k$ is not automatically rejected. Instead, an acceptance rule known as the Metropolis criterion (Metropolis et al., 1953) is considered. It is based on a probability quantity

$$p = \exp\left(-\Delta S_k / T\right), \tag{8}$$

where T is a user-defined control parameter called *temperature*. From equation (8, we see that lower temperatures and/or larger differences, in the function values decrease the probability of a downhill move. In a probabilistic manner, the Metropolis criterion allows, thus, to jump away from a local maximum, so as to eventually reach the region where the global maximum is located. In order to visit as densely as possible the objective function after a given number of steps, the step-length vector $\mathbf{v}$ is adjusted so that at about one-half of the total number of moves are accepted.

After a certain number of cycles of moves along every direction within the search space and with a predefined number of step-length adjustments, a temperature reduction is imposed by means of the relation

$$T^{'} = \mu T, \tag{9}$$

where μ is the temperature reduction factor. As the temperature declines, downhill moves are less likely to be accepted. As a consequence, the number of rejections increases and the step-length decreases. The algorithm focuses, thus, on the most promising area. Of course, the crux of the method lies on the choice of the initial and subsequent temperatures, as well as the selected acceptance criterion.

The algorithm stops when, according to a user-selected criterion, no improvements on the function values are obtained, the last function value being declared the global maximum and the corresponding parameters declared the optimum parameters. In the CRS problem, to avoid a time consuming with this stopping criteria, the process can be interrupted when a predefined maximum number of function evaluations is reached.

APPENDIX B

QUASI-NEWTON

We finally provide a brief description of the Quasi-Newton (QN) method, that has been applied to refine the initial CRS parameters previously obtained using the SA approach. As well known, the QN method is a powerful approach designed to find a local extremum of a given objective function. A number of algorithms exist that implement the QN method. In this paper, we have considered the so-called BFGS (Broyden-Fletcher-Goldfarb-Shannon) algorithm. For a comprehensive description and discussion of optimization methods, including the present QN procedure, the reader is referred to Gill et al. (1981). The simplest way to introduce the QN method is consider, as a first step, the conceptually easier Newton's Method. As seen below, the QN method is a variation of Newton's method that offers in many cases significant computational advantages. Newton's method is an iterative algorithm designed to find the extremum of an objective function based on successive quadratic approximations of that function. For a given initial point (vector parameter), $\mathbf{m}_o$, the second-order Taylor expansion of the semblance, $S(\mathbf{m})$ at a point $\mathbf{m}$ and in the vicinity of $\mathbf{m}_o$, is given by

$$S(\mathbf{m}) = S(\mathbf{m}_o) + \mathbf{g}_o \cdot (\mathbf{m} - \mathbf{m}_o) + \frac{1}{2}(\mathbf{m} - \mathbf{m}_o) \cdot \mathbf{H}_o(\mathbf{m} - \mathbf{m}_o), \tag{10}$$

where, $\mathbf{g}_o$ and $\mathbf{H}_o$ are the gradient vector and the Hessian matrix of the function evaluated at $\mathbf{m}_o$, respectively. A condition for a point $\mathbf{m}$ to be an extremum of the objective function is that the gradient of that function vanishes at $\mathbf{m}$ (i.e.,$\nabla S(m) = 0$). Applying this condition to the approximation (10) yields the result

$$\mathbf{m} = \mathbf{m}_o - \mathbf{d}_o \ , \quad \text{with } \mathbf{H}_o]\mathbf{d}_o = \mathbf{g}_o. \tag{11}$$

Newton's method uses the above simple considerations to formulate the following iterative process designed to determine a local extremum of the objective function, $S(\mathbf{m})$: For a given initial point, $\mathbf{m}_o$ at which the gradient, $\mathbf{g}_o$ and Hessian matrix, $\mathbf{H}_o$, of the objective function are computed, define the sequence, $\{\mathbf{m}_k\}$, determined by the recursion

$$\mathbf{m}_{k+1} = \mathbf{m}_k - \mathbf{d}_k \ , \quad \text{with } \mathbf{H}_k\mathbf{d}_k = \mathbf{g}_k. \tag{12}$$

Here, $\mathbf{g}_k$ and $\mathbf{H}_k$ are the gradient and Hessian matrix of the semblance function, respectively, computed at the point $\mathbf{m}_k$. Under suitable conditions satisfied by the objective function, the procedure converges to the extremum. Note that Newton's method is a local optimization scheme, namely it finds the extremum that is "close" to the given initial point.

Newton's method may become too expensive, because in most cases the Hessian matrix evaluations require large computational effort. The Quasi-Newton (QN) method is designed to overcome this difficulty by replacing the original Hessian matrices by suitable approximation matrices, that are more easily evaluated. These Hessian matrix approximations are recursively obtained using function values and gradients determined by previous iterations. A typical QN recursion scheme can be written in the following form (compare with the corresponding Newton's recursion of equation (12)): Given the point $\mathbf{m}_k$, its gradient, $\mathbf{g}_k$, and its approximated Hessian matrix, $\tilde{\mathbf{H}}_k$, define the next iterate by

$$\mathbf{m}_{k+1} = \mathbf{m}_k - \alpha_k\mathbf{d}_k \quad \text{with } \tilde{\mathbf{H}}_k\mathbf{d}_k = \mathbf{g}_k. \tag{13}$$

in which α_k is a scalar called the step length. The quantity α_k is a somewhat empirically selected so as to insure that the condition

$$S(\mathbf{m}_{k+1}) = S(\mathbf{m}_k - \alpha_k\mathbf{d}_k) > S(\mathbf{m}_k) \tag{14}$$

is satisfied. Equation (14) simply means that the objective function increases its value when we move from $\mathbf{m}_k$ to $\mathbf{m}_{k+1}$. Having obtained the new point, $\mathbf{m}_{k+1}$, we directly determine its corresponding new gradient, $\mathbf{g}_{k+1}$. To complete the iteration procedure, it finally remains to define the new (approximated) Hessian matrix, $\tilde{\mathbf{H}}_{k+1}$. For this, we introduce the notations

$$\mathbf{s}_k = \mathbf{m}_{k+1} - \mathbf{m}_k \quad \text{and} \quad \boldsymbol{\eta}_k = \mathbf{g}_{k+1} - \mathbf{g}_k \ , \tag{15}$$

for the changes of m and g, respectively, in the k-th iteration. The determination of $\mathbf{H}_{k+1}$ requires to satisfy the so-called *secant condition*

$$\tilde{\mathbf{H}}_{k+1}\mathbf{s}_k = \boldsymbol{\eta}_k. \tag{16}$$

A particularly useful updating formula to approximate $\tilde{\mathbf{H}}_{k+1}$ is provided by the BFGS implementation of the QN method. It is given by

$$\tilde{\mathbf{H}}_{k+1} \approx \tilde{\mathbf{H}}_k + \frac{\boldsymbol{\eta}_k\boldsymbol{\eta}_k^T}{\boldsymbol{\eta}_k^T\mathbf{s}_k} - \frac{\tilde{\mathbf{H}}_k\mathbf{s}_k\mathbf{s}_k^T\tilde{\mathbf{H}}_k}{\mathbf{s}_k^T\tilde{\mathbf{H}}_k\mathbf{s}_k}. \tag{17}$$

Equations (13) and (16) or (17) complete the QN iteration procedure.